Isospin influences on particle emission and critical phenomena in nuclear dissociation

Y. G. Ma[1,2,3,*] Q. M. Su,[2] W. Q. Shen,[2] D. D. Han,[4] J. S. Wang,[2] X. Z. Cai,[2] D. Q. Fang,[2] and H. Y. Zhang[2]
[1]*CCAST (World Laboratory), P.O. Box 8730, Beijing 100080, China*
[2]*Shanghai Institute of Nuclear Research, Chinese Academy of Sciences, P.O. Box 800-204, Shanghai 201800, China*[†]
[3]*T.D. Lee Physics Laboratory, Fudan University, Shanghai 200433, China*
[4]*Electric Engineering Department, East China Normal University, Shanghai 200061, China*
(Received 12 February 1999; published 22 July 1999)

Features of particle emission and critical point behavior are investigated as functions of the isospin of disassembling sources and temperature at a moderate freeze-out density for medium-size Xe isotopes in the framework of the isospin-dependent lattice gas model. Multiplicities of emitted light particles, isotopic, and isobaric ratios of light particles show the strong dependence on the isospin of the dissociation source, but double ratios of light isotope pairs and the critical temperature determined by the extreme values of some critical observables are insensitive to the isospin of the systems. Values of the power law parameter of cluster mass distribution, mean multiplicity of intermediate mass fragments (IMF), information entropy, and Campi's second moment also show a minor dependence on the isospin of Xe isotopes at the critical point. In addition, the slopes of the average multiplicities of the neutrons (N_n), protons (N_p), charged particles (N_{CP}), and IMFs (N_{IMF}), slopes of the largest fragment mass number ($A_{\max}$), and the excitation energy per nucleon of the disassembling source (E^*/A) to temperature are investigated as well as variances of the distributions of N_n, N_p, N_{CP}, N_{IMF}, $A_{\max}$, and E^*/A. It is found that they can be taken as additional judgements to the critical phenomena. [S0556-2813(99)02108-1]

PACS number(s): 25.70.Pq, 05.70.Jk, 24.10.Pa, 24.60.Ky

I. INTRODUCTION

Isospin influence on the formation and decay of hot nuclei is an important subject in heavy ion collision physics nowadays. Interest in this direction has been largely pushed away with the development of the radioactive beam technique. Many new impressive experiments aiming at exploring such isospin effects can be performed by using the radioactive beams and/or targets with large neutron or proton excess. They offer the possibility to study the properties of nuclear matter in the range from symmetrical nuclear matter to pure neutron matter. Recently some theoretical investigations of the nuclear equation of state, chemical and mechanical instabilites, as well as liquid-gas phase transition for isospin asymmetrical nuclear matter have been performed [1]. In addition, the study of the isospin-dependent nucleon-nucleon cross section [2–5] is also an important subject due to its significant effect on the dynamical process of heavy ion reactions induced by radioactive beams. Experimentally some new isospin-dependent phenomena have also been discovered. For examples, the isospin dependences of preequilibrium nucleon emission [6–9], nuclear stopping [10], nuclear collective flow [11,12], the total reaction cross section, radii of neutron-rich nuclei [13–15], and subthreshold pion production [16] have been studied by several groups. However, more experimental and theoretical studies are still needed to better understand the isospin physics.

On the other hand, the phase transition and critical point behavior in a finite nuclear system is a topic open to debate. Two kinds of important phase transitions of nuclear matter, namely, the liquid gas phase transition and the quark-gulon plasma phase transition which have been predicted to occur in HIC in the intermediate and ultrarelativistic energy domains, respectively, are attracting more and more nuclear scientists. Due to the manifest significance of both phase transitions in clarifing the properties of nuclear matter in extreme conditions, theoretical physicists are trying to present various possible judgements to characterize the phase transition with diverse models. Experimentalists are searching for such evidence with the help of advanced and complicated setups.

In this article, we will investigate some isospin effects on cluster emission and the critical point behavior stemming from the nuclear liquid gas phase transition in the framework of the isospin-dependent lattice gas model. The paper is organized as follows. In Sec. II, a brief description of the isospin-dependent lattice gas model is given. Results and discussions for the disassembly of ^{122,129,137,146}Xe isotopes at a fixed freeze-out density of $\sim 0.39\rho_0$ are presented in Sec. III. First, the multiplicities of particle emission are used to discuss the influence of the isospin. In addition, the slopes of some average quantities to temperature and the variances of the distributions of some physical observables are argued to be the judgements to locate the critical point. Secondly, the isospin dependence of the ratios between two light particles (LP's) is investigated. Thirdly, the double ratios between two pair light isotopes are studied. Fourthly, critical observables with different isospins are presented. Finally a summary is given in Sec. IV.

II. DESCRIPTION OF MODEL

The lattice gas model of Lee and Yang [17], where the grand canonical partition function of a gas with one type of

*Corresponding Author. Email address: mayugang@public1.sta.net.cn
†Corresponding address.

atom is mapped onto the canonical ensemble of an Ising model for spin-1/2 particles, has successfully described the liquid-gas phase transition for atomic systems. The same model has already been applied to nuclear physics for isospin symmetrical systems in the grancanonical ensemble [18] with an approximate sampling of the canonical ensemble [19–23], and also for isospin asymmetrical nuclear matter in the mean field approximation [24]. In this article, we will adopt a lattice gas model similar to that developed by Pan and Das Gupta [20,21]. Some details and features of the model can be found in their papers. In comparison with the earlier version of their model [20,21], the differences in this work are that the exact Metropolis sampling for placing nucleons on the cubic lattice are adopted and the isospin-dependent interaction potential is taken (which has also been incarnated in their recent works [25,26]). To better understand the context of this work we will briefly describe the model and Monte Carlo Metrolpois sampling technique.

In the lattice gas model, A nucleons with an occupation number s which is defined $s=1$ (-1) for a proton (neutron) or $s=0$ for a vacancy, are placed on the L sites of lattice. Nucleons in the nearest-neighboring sites have interaction with an energy $\epsilon_{s_i s_j}$. The Hamiltonian is written as

$$E=\sum_{i=1}^{A}\frac{P_i^2}{2m}-\sum_{i<j}\epsilon_{s_i s_j}s_i s_j. \tag{1}$$

The interaction constant $\epsilon_{s_i s_j}$ is fixed to reproduce the binding energy of the nuclei. In order to incorporate the isospin effect in the lattice gas model, the short-range interaction constant $\epsilon_{s_i s_j}$ is chosen to be the difference between the nearest-neighboring like nucleons and unlike nucleons: $\epsilon_{nn}=\epsilon_{pp}=\epsilon_{-1-1}=\epsilon_{11}=0$. MeV, $\epsilon_{pn}=\epsilon_{np}=\epsilon_{1-1}=\epsilon_{-11}=-5.33$ MeV, which indicates the repulsion between the nearest-neighboring like nucleons and the attraction between the nearest-neighboring unlike nucleons. This kind of isospin- dependent interaction incorporates, to a certain extent, the Pauli exclusion principal and effectively avoids producing unreasonable clusters, such as di-protons, di-neutrons, etc. A three-dimensional cubic lattice with L sites is used which results in an assumed freeze-out density of the disassembling system $\rho_f=(A/L)\rho_0$, in which ρ_0 is the normal nuclear density. The disassembly of the system is to be calculated at ρ_f, beyond which nucleons are too far apart to interact. $N+Z$ nucleons are put into L sites by Monte Carlo sampling using the exact Metropolis algorithm [19,27].

As pointed out in Refs. [28,29], one has to be careful treating the process of Metropolis sampling in order to maintain the detailed balance and therefore warrant the correct equilibrium distribution in the final state. Speaking in detail, in this work, we first establish an initial configuration with $N+Z$ nucleons. Second, for each event, we will test a sufficient number of ''spin-exchange'' steps, e.g., 20 000 steps, to let the system generate states with a probability proportional to the Boltzmann probability distribution with the Metropolis algorithm. In each spin-exchange step, we make a random trial change on the basis of the previous configuration. For example, we choose a nucleon at random and attempt to exchange it with one of its neighboring nucleons or the vacancies at random regardless of the sign of its spin (Kawasaki-like spin-exchange dynamics [30]). Then we compute the change ΔE in the energy of the system due to the trial change. If ΔE is less than or equal to zero, we accept the new configuration and repeat the next spin-exchange step. If ΔE is positive, we compute the ''transition probability'' $W=e^{-\Delta E/T}$ and compare it with a random number r in the interval [0,1]. If $r\leqslant W$, we accept the new configuration; otherwise we retain the previous configuration and then start the next spin-exchange step. 20 000 spin-exchange steps are performed to assure that we get the equilibrium state. Third, once the nucleons have been placed stably on the cubic lattice after 20 000 spin-exchange steps for each event, their momenta are generated by Monte Carlo sampling of the Maxwell-Boltzmann distribution. Thus various observables can be calculated in a straightforward fashion for each event. One point that should be emphasized here is that the above Monte Carlo Metropolis spin-exchange approach between the nearest neighbors, independent of their spin, is evidenced to be satisfied by the detailed balance as noted in Refs. [28,29]. In other words, this sampling method will guarantee that the generated microscopic states form an equilibrium canonical ensemble.

One of the basic measurable quantities is the size distribution of clusters. The definition of clusters has been extensively discussed in Refs. [20–22]. The first method is the so-called Ising cluster method which combines all the connected sites as a cluster. However, it is not a proper approach to define clusters in the lattice gas model since it does not fulfill the requirement that the correlation length should diverge at the critical point [22]. In condensed matter physics, Coniglio and Klein [31] proposed to combine the above site percolation with an addition bond percolation algorithm using a temperature-dependent bonding probability $p(T)=1-e^{-\epsilon_{s_i s_j}s_i s_j/2T}$. In the lattice gas model, a similar way to Coniglio and Klein's prescription is extensively adopted to define the cluster [20–23]: i.e., two neighboring nucleons are viewed to be in the same fragment if their relative kinetic energy is insufficient to overcome the attractive potential $P_r^2/2\mu-\epsilon_{s_i s_j}s_i s_j<0$. This results in a similar temperature-dependent bonding probability as in Coniglio and Klein's prescription.

III. RESULTS AND DISCUSSIONS

Four isotopes of Xe are chosen as examples to illustrate the isospin effect with the help of the isospin-dependent lattice gas model. Their isospin parameters $[I=(N-Z)/A]$ are about 0.11, 0.16, 0.21, and 0.26 for ^{122}Xe, ^{129}Xe, ^{137}Xe, and ^{146}Xe, respectively. The freeze-out density ρ_f has been chosen to be close to 0.39 ρ_0, as extracted from the analysis of Ar+Sc [20] and ^{35}Cl+Au and ^{70}Ge+Ti [32] with the same model. There is also good experimental support that the value of ρ_f is significantly below $0.5\rho_0$ [33]. 343 sites with $7\times7\times7$ cubes result in 0.36, 0.38, 0.40, and 0.43 ρ_0 of the freeze-out density ρ_f for ^{122,129,137,146}Xe, respectively. Calculations were performed from 3 to 7 MeV with a step of 0.5

MeV and 1000 events were accumulated at each temperature for each isotope.

A. Cluster emission and its application to locate the critical temperature

1. Multiplicity of clusters, the largest fragment mass, and excitation energy

Before presenting the calculated results, we first introduce a definition of the excitation energy in this lattice gas model. The excitation energy per nucleon can be written as [21]

$$E^*/A = E_T - E_{\mathrm{g.s.}} = \left(\frac{3}{2}T + \epsilon_{np}\frac{N_{np}^{T}}{A}\right) - \epsilon_{np}\frac{N_{np}^{\mathrm{g.s.}}}{A}, \qquad (2)$$

where $N_{np}^{\mathrm{g.s.}}$ and N_{np}^{T} are the number of the bonds of unlike nucleons in the ground state (zero temperature) and at T, respectively. Experimentally the excitation energy of a nuclear system is generally given with respect to a cold ($T=0$) nucleus at normal nuclear density. In this classical model, we adopt a similar definition for the ground state, i.e., it corresponds to a cold nucleus at zero temperature and normal nuclear density where there is no kinetic energy so that the ground state energy per nucleon is $-\epsilon_{np}(N_{np}^{\mathrm{g.s.}}/A)$. $N_{np}^{\mathrm{g.s.}}$ is determined by the geometry and is taken as the maximum bond number of unlike nucleons for a disassembling source as it approaches zero temperature and normal nuclear density.

Figure 1 shows the average multiplicites of the emitted neutrons, protons, charged particles, and intermediate mass fragments, the average values of the largest fragment masses, and the average excitation energies per nucleon of the disassembling source as functions of temperature and isospin. At the point of temperature dependence, N_n, N_p, N_{CP}, and E^*/A increase while $A_{\max}$ decreases with temperature as expected. However, N_{IMF} shows a rise and fall with temperature as seen in previous studies [34–37], which has been explained by the onset of the multifragmentation. At the point of isospin dependence, N_n shows a positive correlation with I which is obviously reasonable due to the larger number of neutrons for isotopes with larger I. Similarly, N_{IMF} and $A_{\max}$ show minor positive correlation with I. Reversely, N_p, N_{CP}, and E^*/A seem to have anticorrelation with I at the same temperature even though the same number of protons are started with in these dissociation isotopic sources. Experimentally, similar pictures for free neutrons and protons were found in $^{32}\mathrm{S}+^{144,154}\mathrm{Sm}$ reactions [38]. How do we understand these phenomena?

Two interpretations seem to be possible. On the one hand, the symmetrical potential term in Eq. (1) will play an important role in controlling the emission of nucleons and clusters. With the increase of the isospin of the sources, protons will feel a stronger attractive potential due to the neighboring neutrons sharing similar increases which results in more bound protons for disassembling sources with higher isospins. Vice versa, neutrons will, on one side, feel the stronger repulsive interaction due to more neutron-neutron pairs and, on the other side, feel a smaller attractive potential because of the decrease of the average assortative number of nearest-neighboring protons for a certain neutron with the increase of the isospins of the sources. Both reasons will lead to the production of more unbound neutrons for disassembling sources with higher isospins. This explanation is similar to the explanation of nucleon emission in the isospin-dependent transport model [1]. However, another interpretation based on the excitation energy seems to be possible, too. In a previous work we explored the idea that the excitation energy can be viewed as a scaling quantity to control nuclear disassembly [39]. We made the mapping from T to E^*/A [see Fig. 1(f)] and replotted N_n, N_p, N_{CP}, N_{IMF}, and $A_{\max}$ as a function of excitation energy per nucleon instead of temperature in Fig. 2. Clearly, the rule for average multiplicity of neutrons is not changed, i.e., the higher the excitation energy and/or isospin, the larger N_n. But for protons, charged particles, intermediate mass fragments, and the largest fragment masses, their average values for four isotopes nearly merge into single curves. In this case, the role of the symmetrical potenial is transferred to the excitation energy of different sources and the isospin dependence of N_p, N_{CP}, N_{IMF}, and $A_{\max}$ at the same temperature shown in Figs. 1(b)–1(e) is nothing but the excitation energy dependence.

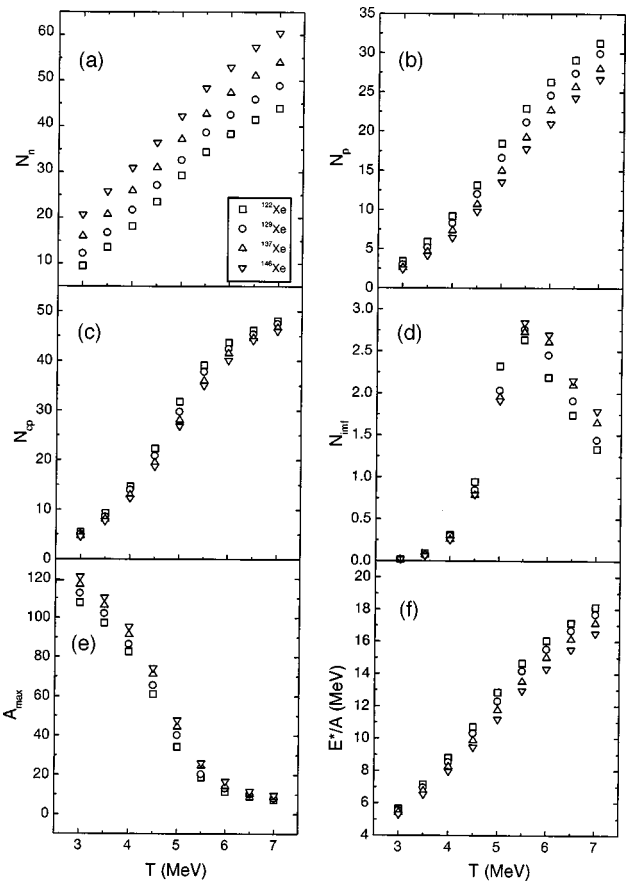

FIG. 1. Average multiplicities for emitted neutrons (a), protons (b), charged particles (c), intermediate mass fragments (d), average values of the largest fragment masses (e), and of excitation energies per nucleon (f) as functions of the temperature and isospin of Xe.

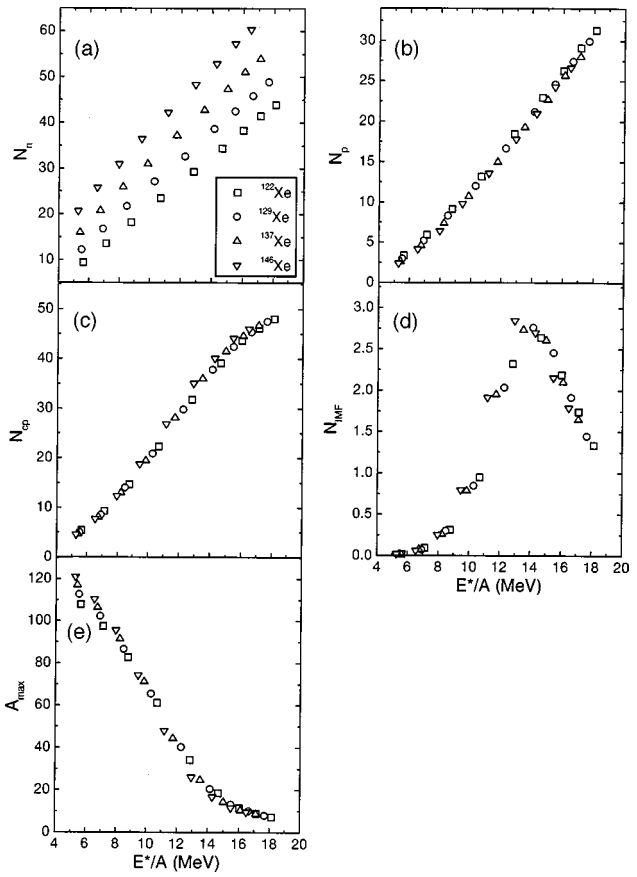

FIG. 2. The same as Fig. 1 but as a function of excitation energy instead of temperature.

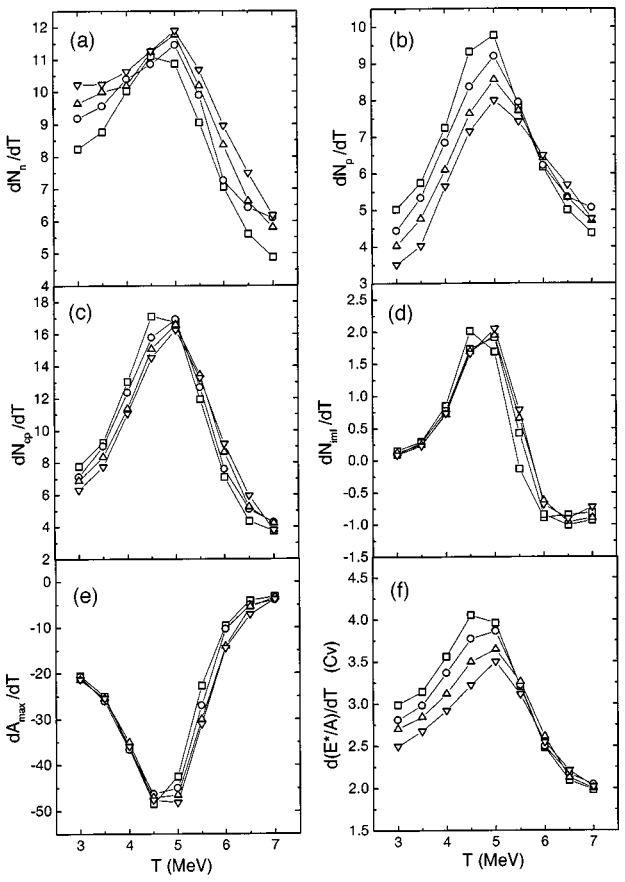

FIG. 3. Slopes of N_n (a), N_p (b), N_{CP} (c), N_{IMF} (d), and $A_{\max}$ (e) to temperature. The symbol is the same as in Fig. 1

2. Slopes of average values to temperature

In Fig. 1 the average values of most physical quantities increase or decrease monotonically with temperature except for the IMF. Is it possible to obtain much information from this figure? Figure 3 gives slopes of N_n, N_p, N_{CP}, N_{IMF}, $A_{\max}$, and E^*/A to temperature. Obviously, each slope has a peak or valley around $T\sim 5$ MeV. At such a turning temperature, some features appear. (1) The emission of light particles and complex fragments increases rapidly within a narrow temperature range, reflecting that the phase space is opening in the largest extent in that time. (2) The decrease of the largest fragment size reaches the valley value for such a finite system. Physically the largest fragment is simply related to the order parameter $\rho_l-\rho_g$ (the difference of density in the liquid and gas phases). In infinite matter, the infinite cluster exists only on the liquid side of the critical point. In finite matter, the largest cluster is present on both sides of the critical point. In this calculation, a valley for the slope of $A_{\max}$ to temperature may correspond to a sudden disappearance of the infinite cluster (bulk liquid) near the critical temperature. (3) The specific heat C_v/A [i.e., $\partial(E^*/A)/\partial T$] has a peak value for such a finite system. All these features are consistent with the concept of phase transition and critical phenomena according to the thermodynamical theory. Hence, these slopes can be viewed as a characteristic judgement of critical phenomena as other critical observables can be (see Sec. II D). Moreover, the fact that the turning temperatures deduced from these slopes for the four isotopic disassembling sources are located at nearly the same temperature of ~ 5 MeV, independent of the isospin, illustrates that the critical temperature is insensitive to the isospin of the disassembling sources. This conclusion is consistent with the results deduced from other critical observables, as shown below (see Sec. II D).

3. The largest fluctuations

The largest fluctuations are also found around the critical temperature in the same calculation. Figure 4 illustrates the rms width (σ) for the multiplicity distributions of neutrons, protons, charged particles, and intermediate mass fragments, for the distributions of the largest fragment masses and excitation energies per nucleon. The variances of multiplicity distributions of neutrons and protons have maximum values or tends to saturation around 5–5.5 MeV, and the variances for the distributions of CP, IMF, $A_{\max}$, and E^*/A show peaks at the same critical temperature. The peaks in the critical point correspond to the cusp of the variances, i.e., their first order derivations are discontinual across the critical temperature which is also an indication of phase transition [40]. Note that the fluctuation of $A_{\max}$ is related to the compressibility of the system. These features are consistent with the critical point behavior where the largest fluctuation should be in terms of statistical theory. Similarly to the results of

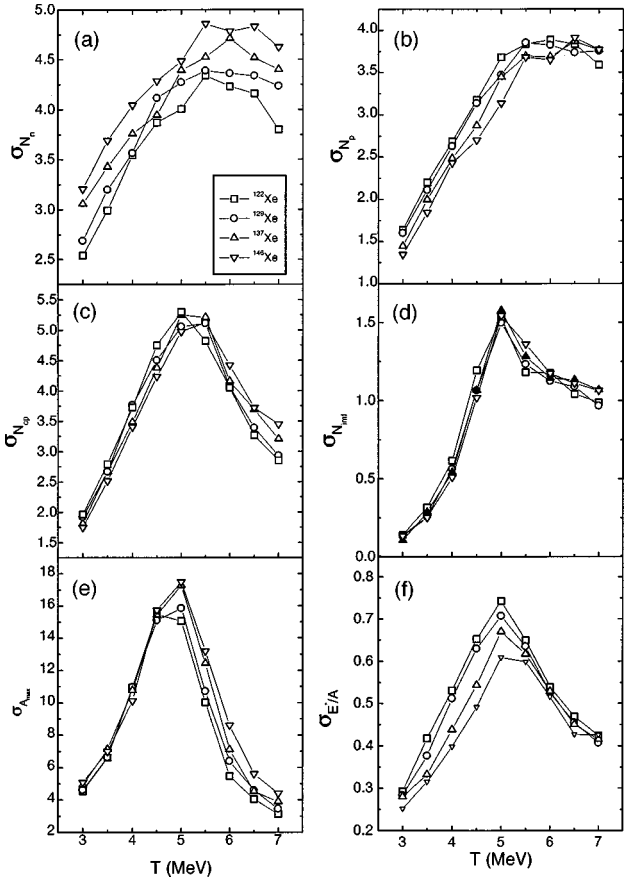

FIG. 4. Variances for the distributions of N_n (a), N_p (b), N_{CP} (c), N_{IMF} (d), $A_{\max}$ (e), and E^*/A (f) versus temperature.

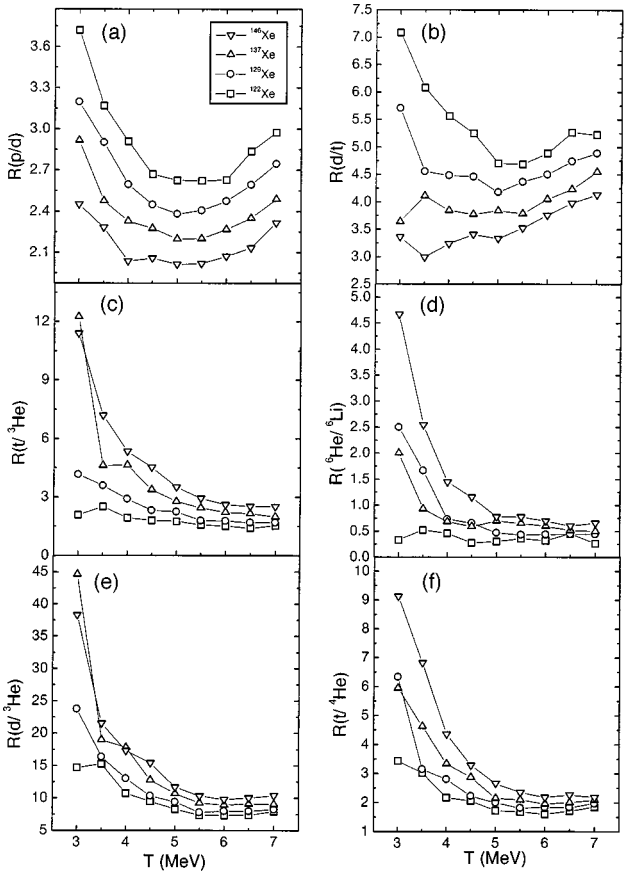

FIG. 5. Isotopic ratios $R(p/d)$ (a) and $R(d/t)$ (b), isobaric ratios $R(t/^3\mathrm{He})$ (c), and $R(^6\mathrm{He}/^6\mathrm{Li})$ (d), and ratios $R(d/^3\mathrm{He})$ (e), and $R(t/^4\mathrm{He})$ (f), as functions of the temperature and isospin of Xe.

slopes, the deduced critical temperature from the largest fluctuation is almost the same regardless of the isospin of the dissociation sources.

B. Ratios between two light particles

In addition to the multiplicity of emitted particles, the ratio between two light particles is probably suitable for investigating the isospin effect. Figure 5 shows the temperature dependences of the isotopic ratios $R(p/d)$ between the yield of protons to that of deuterons and $R(d/t)$ between the yield of deuterons to that of triton and the isobaric ratios $R(t/^3\mathrm{He})$ between the yield of triton and that of helium-3 and $R(^6\mathrm{He}/^6\mathrm{Li})$ between the multiplicity of helium-6 to that of lithium-6, and the ratios $R(^A_Z X/^{A+1}_{Z+1} Y)$ between the light particles having one proton and mass number difference: $R(d/^3\mathrm{He})$ between the multiplicity of deuterons and helium-3 and $R(t/^4\mathrm{He})$ between the multiplicity of triton to that of helium-4 for the disassembly of Xe. For the isotopic ratios $R(p/d)$ and $R(d/t)$, the particle in the denominator has one more neutron than that in the numerator, i.e., the ratios could reflect how neutron poor the products are. Clearly, these ratios decrease with the increase of isospins as shown in Figs. 5(a) and 5(b). It is consistent with the N/Z systematics of the disassembling source. $R(p/d)$ and $R(d/t)$ exist in a wide valley around 5 MeV and then increase with temperature above 5 MeV (near the critical temperature). A similar result was observed experimentally in energetic Au +Au collisions [41]. These results are qualitatively consistent with a rise and fall in the relative production of IMFs, as shown above [see Fig. 1(d)] [34–37]. In a simple coalescence picture this is consistent with a lower baryon density at freeze-out for the most violent collision and disassembly [41]. For the isobaric ratios $R(t/^3\mathrm{He})$ and $R(^6\mathrm{He}/^6\mathrm{Li})$, the particle in the denominator has one more proton than that in the numerator, i.e., the ratio will indicate how neutron rich the products are. Figures 5(c) and 5(d) illustrates that the larger the isospin, the higher the ratios. The N/Z of the emitter has the same trend too. The values of the ratios saturate at higher temperature. For the ratios $R(d/^3\mathrm{He})$ and $R(t/^4\mathrm{He})$, the particle in the denominator has the same number of neutrons as that in the numerator but has one more proton, i.e., this ratio can show how proton deficient or neutron rich the products are. Figures 5(e) and 5(f) show that these ratios can also imply the isospin of the emitted source. The dependence of temperature is similar to $R(t/^3\mathrm{He})$ and $R(^6\mathrm{He}/^6\mathrm{Li})$. In addition to the above ratios, another understandable quantity is the ratio of the yield of emitted neutron to protons $R(n/p)$ (not plotted here because both multiplicities of neutrons and protons have been shown in Fig. 1), which increases with the isospin of the source and tends to saturate at higher temperature.

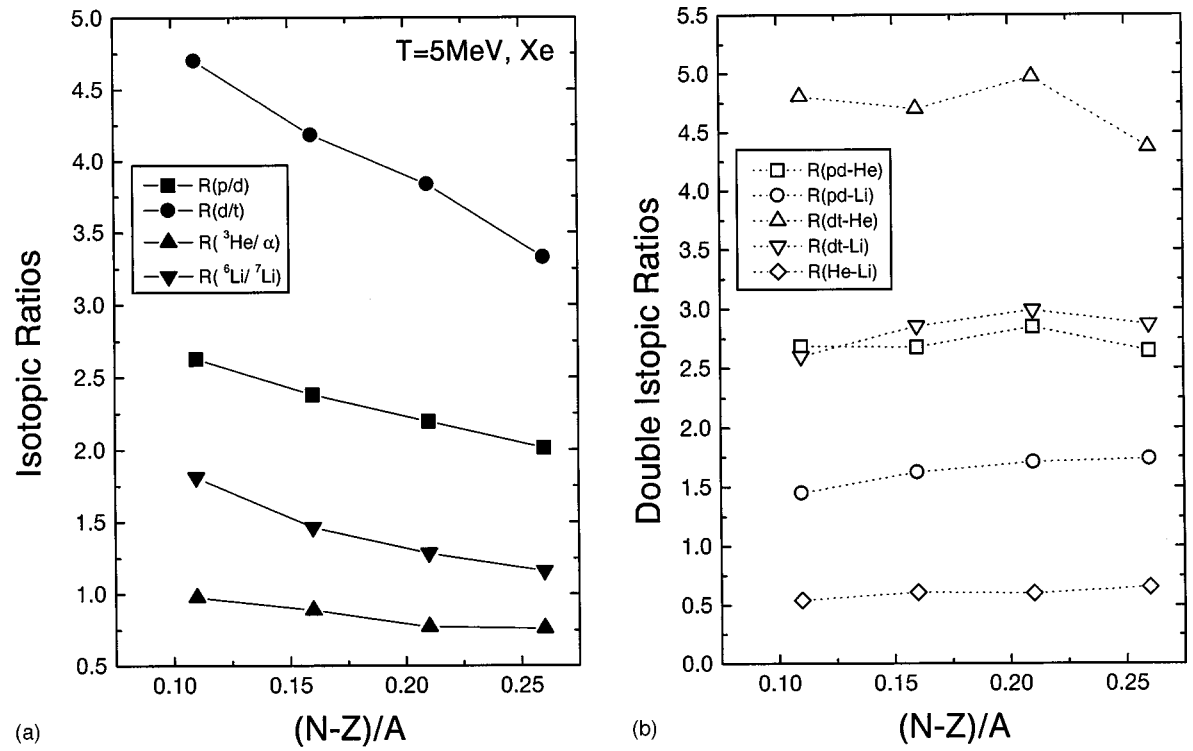

FIG. 6. Isotopic ratios of $R(p/d)$, $R(d/t)$, $R(^3\mathrm{He}/\alpha)$, and $R(^6\mathrm{Li}/^7\mathrm{Li})$ (a) and double ratios $R(pd-\mathrm{He})$, $R(pd-\mathrm{Li})$, $R(dt-\mathrm{He})$, $R(dt-\mathrm{Li})$ and $R(\mathrm{He}-\mathrm{Li})$ (b) as a function of the isospin $(N-Z)/A$ around the critical temperature ~ 5 MeV. The symbols are illustrated in (a) and (b), respectively.

In order to display the isospin systematics of the above ratios clearly, we plot the isotopic ratios of $R(p/d)$, $R(d/t)$, $R(^3\mathrm{He}/\alpha)$, and $R(^6\mathrm{Li}/^7\mathrm{Li})$ as a function of the isospin I at a fixed temperature, e.g., around the critical temperature ~ 5 MeV, in Fig. 6(a). Obviously all the ratios decrease with $(N-Z)/A$ which is consistent with the isospin systematics of disassembling sources.

C. Double ratios between two pair light isotopes

After investigating the multiplicities of LPs and the ratios between one pair of LPs, it is interesting to study the double ratios between two pairs of LPs. With the assumption of thermal and chemical equilibrium, Albergo *et al.* [42] derived a formula of temperature using the double ratios of isotopes. The double ratios of isotopes can cancel out chemical potential effects and offer a particularly promising technique of temperature determination [43–50]. But due to side feeding of light particles of excited primary fragments and other complicated effects in experimental measurements, the temperature from the double ratio must be determined carefully [48,51–53]. However, here we restrict ourselves to a discussion of the double ratios between different light isotopes rather than the isotopic temperature.

Figure 6(b) shows the double ratios between two pair isotopic ratios, namely, $R(pd-\mathrm{He})$ $N_p/N_d/N_{^3\mathrm{He}}/N_{^4\mathrm{He}}$, $R(pd-\mathrm{Li})=N_p/N_d/N_{^6\mathrm{Li}}/N_{^7\mathrm{Li}}$, $R(dt-\mathrm{He})=N_d/N_t/N_{^3\mathrm{He}}/N_{^4\mathrm{He}}$, $R(dt-\mathrm{Li})=N_d/N_t/N_{^6\mathrm{Li}}/N_{^7\mathrm{Li}}$, and $R(\mathrm{He}-\mathrm{Li})=N_{^3\mathrm{He}}/N_{^4\mathrm{He}}/N_{^6\mathrm{Li}}/N_{^7\mathrm{Li}}$. In contrast to the isotopic ratios of Fig. 6(a), the isospin effect of double ratios is washed out as shown in Fig. 6(b). The same picture was found experimentally in central collisions of $^{112}\mathrm{Sn}+^{112}\mathrm{Sn}$ and $^{124}\mathrm{Sn}+^{124}\mathrm{Sn}$ at 40 MeV/nucleon and intepreted with the expanding emitting source model [54]. This independence of isospin is consistent with the attainment of full chemical equilibrium for each disassembling source at a common temperature, which probably reflects that Albergo's temperature is insensitive to the isospin of the system.

D. Fragment distribution and related critical observables

1. Fragment distribution

In light of previous studies on the fragment distribution, we will use observables based on the fragment to signal the onset of the phase transition, e.g., the effective power law parameter τ, the second moment S_2 of fragment distribution, and the informtaion entropy. Before presenting these critical observables, the mass distribution of fragments are shown at $T=4$, 5, 6, and 7 MeV for $^{129}\mathrm{Xe}$ in Fig. 7. Clearly the disassembly mechanism evolves with the nuclear temperature. A few light clusters are emitted and the big residue reserves are at $T=4$ MeV which indicates a typical evaporation mechanism. With increasing temperature, the shoulder of the mass distribution of clusters occurs due to the competition between the fragmentation and the evaporation. This shoulder disappears and the mass distribution becomes a power law shape at $T=6$ MeV, corresponding to the multifragmentation region. When the temperature becomes much higher, the mass distribution becomes much steeper indicating that the disassembling process becomes more violent.

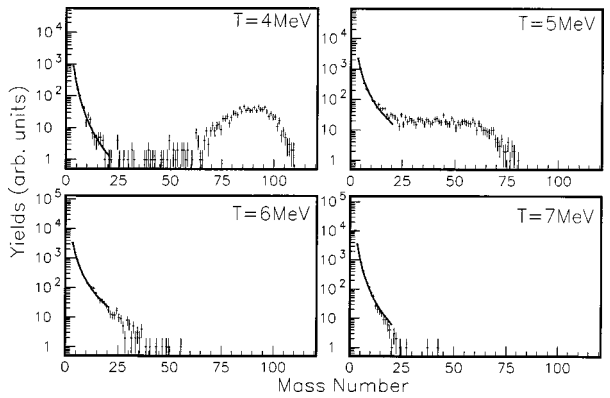

FIG. 7. Mass distribution of ^{129}Xe at $T=4$, 5, 6, and 7 MeV. The lines are the power-law fit.

Power law fits $Y(A)\propto A^{-\tau}$ for these mass distributions have been introduced in Fig. 7 (shown by the lines).

2. Effective power law parameter

It has already been observed that a minimum of power law parameter $\tau_{\min}$ exists if the critical behavior takes place [55,56]. Figure 8(a) displays the τ parameter as a function of temperature for Xe nuclei with different isospins. The minimums of τ parameters in Fig. 8(a) are located close to 5.5 MeV for all the systems, which illustrates its minor dependence on the isospin. In other words, there could be a universal scaling for the mass distribution regardless of the size of the disassembling source when the critical phenomena takes place. However, τ parameters show different values outside the critical region for nuclei with different isospins, e.g., τ decreases with isospin when $T>5.5$ MeV (multifragmentation region).

3. Campi's second moment

In Fig. 8(b) we give the temperature dependences of Campi's second moment of the fragment mass distribution [57], which is defined as

$$S_2=\frac{\sum_{i\neq A\max} A_i^2 n_i(A_i)}{A}, \tag{3}$$

where $n_i(A_i)$ is the number of clusters with A_i nucleons and the sum excludes the largest cluster $A_{\max}$, where A is the mass of the system. At the percolation point S_2 diverges in an infinite system and is maximum in a finite system. Figure 8(b) gives the maximums of S_2 around 5.5 MeV for different isotopes. Again, the critical behavior occurs at the same temperature, independent of the isospin, as τ reveals.

4. Information entropy

Figure 8(c) plots the information entropy H as a function of temperature for Xe isotopes. The information entropy was introduced by Shannon for the first time, in information theory [58]. In high energy collisions, multiparticle production proceeds in the maximum stochasticity, i.e., they should

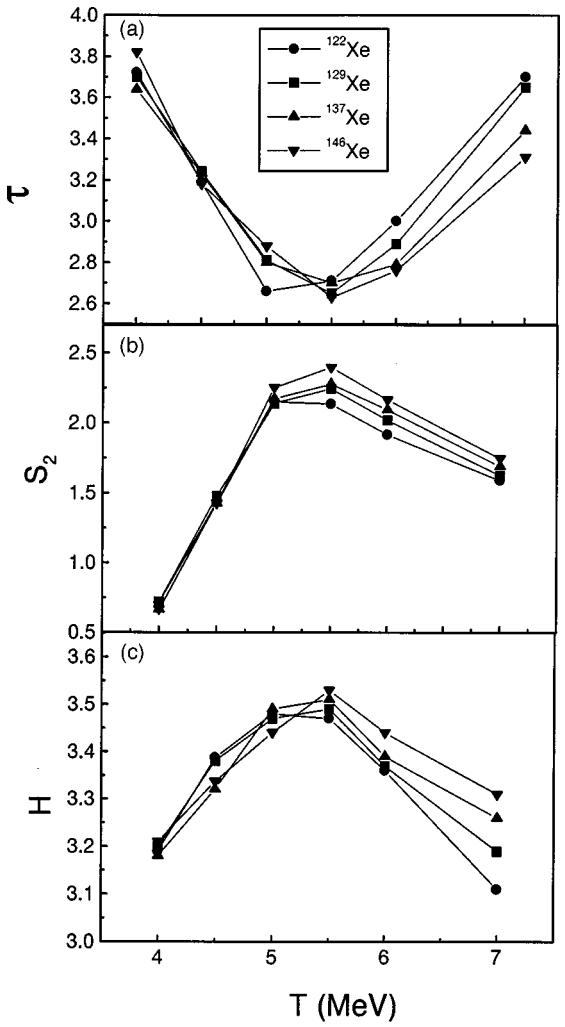

FIG. 8. Critical observables: τ parameter from the power law fit to mass distribution (a), Campi's second moment (b), and information entropy (c) as functions of the temperature and isospin of disassembling sources.

obey the maximum entropy principal. This kind of stochasticity can be quantified via the information entropy. In the different physical condition restraint, the information entropy can be defined with different stochastic variables. For example, the information entropy for particle multiplicity can be defined as

$$H=-\sum_i p_i \ln(p_i). \tag{4}$$

Here p_i can be defined as an event probability having i produced particles and the sum is taken over all multiplicities of products from the disassembling system. H reflects the capacity of the information or the extent of disorder. Here we introduce this entropy for the first time into the search for the liquid gas phase transition and critical phenomenon in the nuclear disassembly. Figure 8(c) shows that the entropy H has peaks close to 5.5 MeV for all isotopes. These peaks indicate that the opening of the phase space in the critical point is the largest. In other words, the system at the critical

temperature has the largest fluctuation and stochasticity which leads to the largest disorder and particle production rate. Beyond the critical point, the information entropy H increases with the isospin.

5. Caloric curve and specific heat

Other direct quantities to illustrate the phase transition are the caloric curve and specific heat. For ideal infinite nuclear matter the first order liquid gas phase transition will reveal a temperature plateau in a wide range of excitation energy, which corresponds to an infinite specific heat at this constant temperature. But for finite nuclear matter the plateau of the caloric curve and the sharpness of the specific heat will be largely smoothed. We assume that the specific heat might keep the imprint of the phase transition well and will probably reveal a salience with the temperature when the phase transition and critical behavior holds. Exchanging the X and Y axes of Fig. 1(f), the so-called caloric curves for Xe isotopes are obtained. For such finite nuclear systems, caloric curves indicate that the temperature increases generally with the excitation energy but a temperature plateau domain is always absent in this lattice gas model. On the other hand, at a fixed temperature, the excitation energy per nucleon decreases with the isospin of dissociation isotopic sources, which is related to the bond numbers of unlike nucleons. Qualitatively, the higher the isospin of the disassembling isotopic source, the larger the N_{np}^{T} and the smaller the excitation energy per nucleon in terms of Eq. (2). Due to the fact that the caloric curves are not linear, the slopes of excitation energy to temperature for these curves, i.e., the specific heat per nucleon at constant freeze-out volume (or density) C_v/A for Xe isotopes is useful to locate the critical point. Figure 3(f) shows that definite peaks of C_v/A exist around 5 MeV for each disassembling source, corresponding to the onset of the critical point behavior. Due to the influence of isospin on the caloric curves, C_v/A shows a similar anticorrelation with isospin especially below the critical temperature.

IV. SUMMARY

In conclusion, the isospin effects of particle emission and critical point behavior were explored for Xe isotopes at a fixed moderate freeze-out density in the framework of the isospin-dependent lattice gas model. Four probes were used to investigate such an effect. The first probe was the multiplicities of LPs, such as N_n and N_p, the multiplicities of charged particles N_{CP} and of intermediate mass fragments N_{IMF}, and the average mass for the largest fragments $A_{\max}$ and the mean excitation energy per nucleon E^*/A. The second probe was the ratio between two LPs, namely, isotopic ratios, such as $R(p/d)$ and $R(^3\mathrm{He}/\alpha)$, isobaric ratios, such as $R(t/^3\mathrm{He})$ and $R(^6\mathrm{He}/^6\mathrm{Li})$, or ratios of two light particls between which there exist one proton and mass number difference, such as $R(d/^3\mathrm{He})$ and $R(t/\alpha)$. The third probe was the double ratios between two isotope pairs, such as $R(pd-\mathrm{He})$, $R(pd-\mathrm{Li})$, $R(dt-\mathrm{He})$, $R(dt-\mathrm{Li})$, and $R(\mathrm{He}-\mathrm{Li})$. The fourth probe was the critical observables, such as the effective power law parameter τ, the information entropy H, the Campi's second moment S_2, the caloric curves, and the specific heat per nucleon C_v/A. The calculation illustrates that N_n, N_p, and ratios of light particles show strong dependences on the isospin of the dissociation source, but this is not the case for the double ratios of light isotopes. The former directly reflects the chemical composition of the source and the latter indicates the chemical equilibrium of the source, which is not self-contradicting but reflects features of the sources on different sides. Meanwhile, the critical temperature for a chain isotopes determined by the extreme values of τ, H, and S_2 is also insensitive to the isospin of sources. This conclusion does not contradict the previous studies on the isospin dependence of critical temperature such as that in Ref. [23], where the span of isospins is from symmetrical nuclear matter to pure neutron matter. If we only look at a small span of isospins for the experimentally measurable medium size isotopes, such as $^{122-146}$Xe, the change of critical temperature is neglectable. This conclusion might indicate that it will be difficult to search for the isospin dependence of the critical temperature which signals the liquid gas phase transition for medium size nuclei from an experimental point of view. In addition, values of the power law parameter of the cluster mass distribution, the mean multiplicity of intermediate mass fragments (IMF's), information entropy (H), and Campi's second moment (S_2) also show minor dependences on the isospin of Xe isotopes at the critical point. In contrary, some isospin dependences of the values of τ, H, and S_2 will be revealed outside the critical region. We note that the information entropy has, for the first time, been introduced into the search for the liquid gas phase transition in this work. In addition, the slopes of N_n, N_p, N_{CP}, N_{IMF}, $A_{\max}$, and E^*/A to temperature and the variances of the distributions of these quantities were argued to be additional judgements for critical phenomena. Because of the insensitivity of the critical temperature to the isospin from the extreme values of τ, H, and S_2, the critical temperature deduced from the above slopes and variances also shows independence on the isospin of the disassembling sources. It will be interesting to confront these conclusions with future experiments.

ACKNOWLEDGMENTS

The authors want to acknowledge Dr. Jicai Pan and Dr. S. Das Gupta for help. This work was supported by the National Natural Science Foundation under Grant No. 19725521, the National Natural Science Foundation of China under Grant No. 19705012, the Science and Technology Development Foundation of Shanghai under Grant No. 97QA14038, the Presidential Foundation of the Chinese Academy of Sciences, the Scientific Research Foundation, by the National Human Resource Administration, Education Administration of China, and the Shanghai Government.

[1] B.A. Li, C.M. Ko, and W. Bauer, Int. J. Mod. Phys. E **7**, 147 (1998), and references therein.
[2] B. te Harr and R. Machleidt, Phys. Rev. C **50**, 31 (1994).
[3] G.F. Bertsch, F.E. Brown, V. Koch, and B.A. Li, Nucl. Phys. **A490**, 745 (1998).
[4] G.Q. Li and R. Machleidt, Phys. Rev. C **48**, 1702 (1993); **49**, 566 (1993).
[5] X.Z. Cai, J. Feng, W.Q. Shen, Y.G. Ma, J.S. Wang, and W. Ye, Phys. Rev. C **58**, 572 (1998).
[6] J.F. Dempsey, R.J. Charity, L.G. Sobotka, G.J. Kunde, S. Gaff, C.L. Gelbke, T. Glasmacher, M.J. Huang, R.C. Lemmon, W.G. Lynch, L. Manduci, L. Martin, M.B. Tsang, D.K. Agnihotri, B. Djerroud, W.U. Schroder, W. Skulski, J. Toke, and W.A. Friedman, Phys. Rev. C **54**, 1710 (1996); R. Wada, K.D. Hildenbrand, U. Lynen, W.F.J. Muller, H.J. Rabe, H. Sann, H. Stelzer, W. Trautmann, R. Trockel, N. Brummund, R. Glasow, K. H. Kampert, R. Santo, E. Eckert, J. Pochodzlla, I. Bock, and D. Pelte, Phys. Rev. Lett. **58**, 1829 (1987).
[7] V. Lozhkin and W. Trautman, Phys. Rev. C **46**, 1996 (1992).
[8] G.J. Kunde *et al.*, Phys. Rev. Lett. **77**, 2897 (1992).
[9] B.A. Li, C.M. Ko, and Z.Z. Ren, Phys. Rev. Lett. **78**, 1644 (1997).
[10] S.J. Yennello, B. Young, J. Yee, J.A. Winger, J.S. Winfield, G.D. Westfall, A. Vander Molen, B.M. Sherrill, J. Shea, E. Norbeck, D.J. Morrissey, T. Li, E. Gualeieri, D. Craig, W. Benenson, and D. Bazin, Phys. Lett. B **321**, 15 (1994); H. Johnstone, T. White, J. Winger, D. Rowland, B. Hurst, F. Gimeno-Nogues, D. O'Kelly, and S.J. Yennello, *ibid.* **371**, 186 (1996); B.A. Li and S.J. Yennello, Phys. Rev. C **52**, R1746 (1995).
[11] R. Pak, W. Benenson, O. Bjarki, J.A. Brown, S.A. Hannuschke, R.A. Lacey, B.A. Li, A. Nadasen, E. Norbeck, P. Pogodin, D.E. Russ, M. Steiner, N.T.B. Stone, A.M. Vander Molen, G.D. Westfall, L.B. Yang, and S.J. Yennello, Phys. Rev. Lett. **78**, 1022 (1997); R. Pak, B.A. Li, W. Benenson, O. Bjarki, J.A. Brown, S.A. Hannuschke, R.A. Lacey, D.J. Magestro, A. Nadasen, E. Norbeck, D.E. Russ, M. Steiner, N.T.B. Stone, A.M. Vander Molen, G.D. Westfall, L.B. Yang, and S.J. Yennello, *ibid.* **78**, 1026 (1997).
[12] B.A. Li, Z.Z. Ren, C.M. Ko, and S.J. Yennello, Phys. Rev. Lett. **76**, 4492 (1996).
[13] W.Q. Shen, B. Wang, J. Feng, W.L. Zhan, Y.T. Zhu, and E.P. Feng, Nucl. Phys. **A491**, 130 (1989).
[14] Y.G. Ma, W.Q. Shen, J. Feng, and Y.Q. Ma, Phys. Lett. B **302**, 386 (1993); Phys. Rev. C **48**, 850 (1993).
[15] T. Suzuki, H. Geissel, O. Bochkarev, L. Chgulkov, M. Golovkov, D. Hirata, H. Irnich, Z. Janas, H. Keller, T. Kobayashi, G. Kraus, G. Munzenberg, S. Neumaier, F. Nickel, A. Ozawa, A. Piechaczeck, E. Roeckl, W. Schwab, K. Summerer, K. Yoshida, and I. Tanihata, Phys. Rev. Lett. **75**, 3241 (1995).
[16] S. Nagamiya, M.C. Lemaire, E. Moeller, S. Schnetzer, G. Shapiro, H. Steiner, and I. Tanihata, Phys. Rev. C **24**, 971 (1981).
[17] T.D. Lee and C.N. Yang, Phys. Rev. **87**, 410 (1952).
[18] T.S. Biro, J. Knoll, and J. Richert, Nucl. Phys. **A459**, 692 (1986); S.K. Samaddar and J. Richert, Phys. Lett. B **218**, 381 (1989); Z. Phys. A **332**, 443 (1989).
[19] W.F.J. Müller, Phys. Rev. C **56**, 2873 (1997).
[20] J. Pan and S. Das Gupta, Phys. Lett. B **344**, 29 (1995); Phys. Rev. C **51**, 1384 (1995).
[21] J. Pan and S. Das Gupta, Phys. Rev. C **53**, 1319 (1996).
[22] X. Campi and H. Krivine, Nucl. Phys. **A620**, 46 (1997).
[23] F. Gulminelli and P. Chomaz, Report No. Lpcc 98-05, 1998 (unpublished).
[24] S. Ray, J. Shamanna, and T.T.S. Kuo, Phys. Lett. B **392**, 7 (1997).
[25] S. Das Gupta, J. Pan, I. Kvasnikova, and C. Gale, Nucl. Phys. **A621**, 897 (1997); J. Pan, S. Das Gupta, and M. Grant, Phys. Rev. Lett. **80**, 1182 (1998).
[26] J. Pan and S. Das Gupta, Phys. Rev. C **57**, 1839 (1998); (private communication).
[27] M. Metropolis, A.W. Rosenbluth, M.N. Rosenbluth, A.H. Teller, and E. Teller, J. Chem. Phys. **21**, 1087 (1953).
[28] C.S. Shida and V.B. Henriques, cond-mat/9703198, 1997.
[29] J.M. Carmona, J. Richert, and A. Tarancon, Nucl. Phys. **A643**, 115 (1998).
[30] K. Kawasaki, in *Phase Transition and Critical Phenomena*, edited by C. Domb and M.S. Green (Academic, New York, 1972), Vol. 2.
[31] A. Coniglio and E. Klein, J. Phys. A **13**, 2775 (1980).
[32] L. Beaulieu, D.R. Bowman, D. Fox, S. Das Gupta, J. Pan, G.C. Ball, B. Djerroud, D. Dore, A. Galindo-Uribarri, D. Guinet, E. Hagberg, D. Horn, R. Laforest, Y. Lacochelle, P. Lautesse, M. Samri, R. Roy, and C. St-Pierre, Phys. Rev. C **54**, R973 (1996).
[33] M. D' Agostino, A.S. Botvina, P.M. Milazzo, M. Bruno, G.J. Unde, D.R. Bowman, L. Celano, N. Colonna, J.D. Dinius, A. Ferrero, M.L. Fiandri, C.K. Gelbke, T. Glasmacher, F. Gramegan, D.O. Handzy, D. Horn, W.C. Hsi, M.J. Juang, I. Iori, M.A. Lisa, W.G. Lynch, L. Manduci, G.V. Margagliotti, P.F. Mastinu, I.N. Mishustin, C.P. Montoya, A. Moroni, G.F. Peaslee, F. Petruzzelli, L. Phair, R. Rui, C. Schwarz, M.B. Tsang, G. Vannini, and C. Williams, Phys. Lett. B **37**, 175 (1996).
[34] C.A. Ogilivie, J. C. Adloff, M. Begemann-Blaich, H. Hubele, G. Imme, I. Iori, P. Kreutz, G.J. Kunde, S. Leray, V. Lindenstruth, Z. Liu, U. Lynen, R. J. Meijer, U. Milkau, W.F.J. Muller, C. Ngo, J. Pochodzalla, G. Raciti, G. Rudolf, H. Sann, A. Schutauf, W. Seidel, L. Stuttge, W. Trautmann, and A. Tucholski, Phys. Rev. Lett. **67**, 1214 (1991).
[35] M.B. Tsang, W.C. Hsi, W.G. Lynch, D.R. Bowman, C.K. Gelbke, M.A. Lisa, and G.F. Peaslee, Phys. Rev. Lett. **71**, 1502 (1993); G.F. Peaslee, M.B. Tsang, C. Schwarz, M.J. Huang, W.S. Huang, W.C. Hsi, C. Williams, W. Bauer, D.R. Bowman, M. Charitier, J. Dinius, C.K. Gelbke, T. Glasmacher, D.O. Handzy, M.A. Lisa, W.G. Lynch, C.M. Mader, L. Phair, M.C. Lemaire, S.R. Souza, G. Van Buren, R.J. Charity, L.G. Sobotka, G.J. Kunde, U. Lynen, J. Pochodzalla, H. Sann, W. Trautmann, D. Fox, R.T. de Souza, G. Peilert, W.A. Friedman, and N. Carlin, Phys. Rev. C **49**, R2271 (1994).
[36] Y.G. Ma and W.Q. Shen, Phys. Rev. C **51**, 710 (1995).
[37] Y.G. Ma, Q.M. Su, W.Q. Shen, J.S. Wang, X.Z. Cai, and D.Q. Fang, Chin. Phys. Lett. **16**, 256 (1999).
[38] D. Hilscher, in *Proceedings of a Specialist's Meeting on Preequilibrium Nuclear Reactions*, edited by B. Strohmaier (OECD, Paris, 1988), p. 245.
[39] Y.G. Ma, Q.M. Su, W.Q. Shen, J.S. Wang, X.Z. Cai, D.Q. Fang, H.Y. Zhang, and D.D. Han, Eur. Phys. J. A **4**, 217 (1999).

[40] K.C. Chase and A.Z. Mekjian. Phys. Lett. B **379**, 50 (1996).
[41] L. Ahle, Y. Akiba, K. Ashktorab, M.D. Baker, D. Beavis, H.C. Britt, J. Chang, C. Chawford, Z. Chen, C.Y. Chi, Y.Y. Chu, V. Cianciolo, B.A. Cole, H.J. Crawford, J.B. Cumming, R. Debbe, W. Eldredge, J. Engelage, S.Y. Fung, J.J. Gaardhoje, M. Gonin, S. Gushue, H. Hamagaki, A.G. Hansen, L. Hansen, G. Heintzlman, S. Homma, R.S. Hayano, E. Judd, J.H. Kang, H. Kaneko, A. Kuria, M. Levine, J. Luke, Y. Miake, B. Moskowitz, M. Moulson, S. Nagamiya, M.N. Namboodiri, T.K. Nayak, C.A. Ogilvie, J. Olnes, L.P. Remsberg, T.C. Sangster, R. Seto, K. Shigaki, H. Sako, R. Soltz, S.G. Steadman, G.S.F. Stephans, T. Sung, M.J. Tannenbaum, J.H. Thomas, S.R. Tonse, S. Ueno-Hayashi, F. Videbek, F.Q. Wang, Y. Wang, D.S. Woodruff, Y. Wu, G. Xu, K. Yagi, D. Zachary, W.A. Zajc, F. Zhu, and Q. Zhu, Phys. Rev. C **57**, 1416 (1998).
[42] S. Albergo, S. Costa, E. Costanzo, and A. Rubbino, Nuovo Cimento A **89**, 1 (1985).
[43] J. Pochodzalla, T. Mohlenkamp, T. Rubehn, A. Schuttauf, A. Worner, E. Zude, M. Begemann-Blaich, Th. Blaich, H. Emling, A. Ferrero, C. Gross, G. Imee, I. Iori, G.J. Kunde, W.D. Kunze, V. Lindenstruth, U. Lynen, A. Moroni, W.F.J. Muller, B. Ocker, G. Raciti, H. Sann, C. Schwarz, W. Seidel, V. Serfling, J. Stroth, W. Trautmann, A. Trzcinski, A. Tucholski, G. Verde, and B. Zwieglinski, Phys. Rev. Lett. **75**, 1040 (1995).
[44] J.A. Hauger, G.J. Kunde, P.M. Milazzo, J.D. Diniu, M. Bruno, N. Colonna, M.L. Fiandri, C.K. Gelbke, T. Glasmacher, F. Gramegna, D.O. Handzy, W.C. Hsi, M.J. Huang, M.A. Lisa, W.G. Lynch, P.F. Mastinu, C.P. Ontoya, A. Moroni, G.F. Peaslee, L. Hair, R. Rui, C. Schwarz, M.B. Tsang, G. Vannini, and C. Williams, Phys. Rev. Lett. **77**, 235 (1996).
[45] Y.G. Ma, A. Siwek, J. Péter, F. Gulminelli, R. Dayras, L. Nalpas, B. Tamain, E. Vient, G. Auger, Ch.O. Bacri, J. Benlliure, E. Bisquer, B. Borderie, R. Bougault, R. Brou, J.L. Charvet, A. Chibi, J. Colin, D. Cussol, E. De Filippo, A. Demeyer, D. Dore, D. Durand, E. Ecomard, Ph. Eudes, E. Gerlic, D. Gourio, D. Guinet, R. Laforest, P. Lautesse, J.L. Laville, L. Lebreton, J.F. Lecolley, A. Le Fevre, T. Lefort, R. Legrain, O. Lopez, M. Louvel, J. Lukasik, N. Marie, V. Metivier, A. Ouatizerga, M. Parlog, E. Plagnol, A. Rahman, T. Reposeur, M.F. Rivet, E. Rosato, F. Saint-Laurent, M. Squalli, J.C. Steckmeyer, M. Stern, L. Tassan-got, C. Volant, and J.P. Wieleczko, Phys. Lett. B **390**, 41 (1997).
[46] V. Serfling, C. Schwarz, R. Bassini, M. Begemann-Blaich, S. Fritz, S.J. Gaff, C. Grob, G. Imme, I. Iori, U. Kleinevob, G.J. Kunde, W.D. Kunze, U. Lynen, V. Maddalena, M. Mahi, T. Mohlenkamp, A. Moroni, W.F.J. Muller, C. Nociforo, B. Ocker, T. Odeh, F. Petruzzelli, J. Pochodzalla, G. Raciti, G. Riccobene, F.P. Romano, A. Saija, M. Schnittker, A. Schuttauf, W. Seidel, C. Sfienti, W. Trautmann, A. Trzcinski, G. Verde, A. Worner, Hongfei Xi, and B. Zwieglinski, Phys. Rev. Lett. **80**, 3928 (1998).
[47] P.M. Milazzo, G. Vannini, M. Azzano, D. Fontana, G.V. Margagliotti, P.F. Mastinu, R. Rui, F. Tonetto, N. Colonna, A. Botvina, M. Bruno, M. D'Agostino, M.L. Fiandri, F. Gramegna, I. Iori, A. Moroni, J.D. Dinius, S. Gaff, C.K. Gelbke, T. Glasmacher, M.J. Huang, G.J. Kunde, W.G. Lynch, L. Martin, C.P. Montoya, and H. Xi, Phys. Rev. C **58**, 953 (1998).
[48] M.B. Tsang, W.G. Lynch, H. Xi, and W.A. Friedman, Phys. Rev. Lett. **78**, 3836 (1997).
[49] H. Xi, M.B. Tsang, M.J. Huang, W.G. Lynch, J.D. Dinies, S.G. Gaff, C.K. Gelbke, T. Glasmacher, G.J. Kund, L Martin, C.P. Montoya, M. Azzano, G.U. Margagliotti, P.M. Milazzo, R. Rui, G. Vannini, L. Celano, N. Colonna, G. Tagliente, A. Ferrero, I. Iori, A. Moroni, F. Petruzzelli, and P.F. Mastinu, Phys. Lett. B **431**, 8 (1998).
[50] H. Xi, T. Odeh, R. Bassini, M. Begemann-Blaich, A.S. Botvina, S. Fritz, S.J. Gaff, C. Gros, G. Imme, I. Iori, U. Kleinevos, G.J. Kunde, W.D. Kunze, U. Lynen, V. Maddalena, M. Mahi, T. Mohlenkamp, A. Moroni, W.F.J. Muller, C. Nociforo, B. Ocker, F. Petruzzelli, J. Pochodzalla, G. Raciti, G. Riccobene, F.P. Romano, Th. Rubehn, A. Saija, M. Schnittker, A. Schuttauf, C. Schwarz, W. Seidel, V. Serfling, C. Sfienti, W. Trautmann, A. Trzcinski, G. Verde, A. Worner, and B. Zwieglinski, Z. Phys. A **359**, 397 (1997).
[51] A. Siwek, D. Durand, F. Gulminelli, and J. Péter, Phys. Rev. C **57**, 2507 (1998).
[52] F. Gulminelli and D. Durand, Nucl. Phys. **A615**, 117 (1997).
[53] J.P. Bondorf, A.S. Botvina, and I.N. Mishustin, Phys. Rev. C **58**, R27 (1998).
[54] G. Kunde, S. Gaff, C.K. Gelbke, T. Glasmacher, M.J. Huang, R. Lemmon, W.G. Lynch, L. Manduci, M.B. Tsang, W.A. Friedman, J. Dempsey, R.J. Charity, L.G. Soboktka, D.K. Agnihotri, B. Djerroud, W.U. Schrsder, W. Skulski, and J. Toke, Phys. Lett. B **416**, 56 (1998).
[55] M.E. Fisher, Ann. Phys. (N.Y.) **3**, 255 (1967); Rep. Prog. Phys. **30**, 615 (1967).
[56] T. Li, W. Bauer, D. Craig, M. Cronqvist, E. Gualtieri, S. Hannuschke, R. Lacey, W.J. Llope, T. Reposeur, A.M. Vaner Molen, G.D. Westfall, W.K. Wilson, J.S. Winfield, J. Yee, S.J. Yennello, A. Nadasen, R.S. Tickle, and E. Norbeck, Phys. Rev. Lett. **70**, 1924 (1993).
[57] X. Campi, Phys. Lett. B **208**, 351 (1998).
[58] K.G. Denbigh and J.S. Denbigh, *Entropy in Relation to Uncomplete Knowledge* (Cambridge University Press, Cambridge, 1995).